ON THE EVOLUTION OF MICROSTRUCTURE AND MECHANICAL PROPERTIES DURING UPSETTING PROCESS OF INGOT TO BILLET CONVERSION IN TYPE 316 AUSTENITIC STAINLESS STEEL

Abstract. Manufacturing high value components involves complex and non-linear thermo-mechanical processes to obtain optimum combination of microstructure and mechanical properties required for the final part. Among these, the ingot-to-billet conversion process, involving forging operations of upsetting and cogging, are critical to refine the as-cast coarse, elongated, and dendritic microstructure. In this study, the first stage of the ingot-to-billet conversion process has been investigated, aiming to understand the evolution of microstructure and its dependencies on the forging process parameters in type 316 austenitic stainless steel and improve the industrial manufacturing route. Hot upsetting tests were carried out on cylindrical samples taken out from an industrial-scale ingot. The resulted microstructures were analysed, using advanced image analysis method, for the fraction and distribution of the recrystallised grains. These measurements were correlated to the thermo-mechanical deformation history described by a finite element (FE) model considering the anisotropic behaviour of the material, originated from the preferential grain growth during casting. The results show the strong dependency of recrystallisation behaviour on the initial microstructure of the as-cast material, throughout the upsetting and cogging operations. The results also demonstrate the importance of considering the anisotropic plastic properties in the FE models to effectively predict the material deformation, shape and thermo-mechanical characteristics applied during forging.

1 Introduction

The control of microstructure during the manufacturing process of engineering components is critical to achieve the necessary mechanical properties required for the final application. The thermo-mechanical loads involved during the ingot-to-billet conversion route must permit the complete recrystallisation of the as-cast structure. Thus, accurate characterisation of thermo-mechanical and microstructural properties of the as-cast material are essential to obtain an optimised and economical manufacturing route guaranteeing the quality of the products.

Laboratory-scale tests are used for the material characterisation of small samples (< Ø 20 x 20 mm) since they permit precise measurements of load and displacement under complex thermo-mechanical loads. The experimental results are used to develop and calibrate the constitutive models governing the material thermo-mechanical and microstructural properties (Jonas et al., 2009) (Han et al., 2015). These can then be implemented in Finite Elements (FE) models to design and optimise relevant manufacturing routes for large industrial scale ingots, ranging from a few hundred kilos to several tons (Antolovich and Evans, 2000).

Due to the solidification process of the as-cast material, its microstructure and behaviour are however specific. The microstructure is composed of coarse and elongated dendritic grains with a preferential crystallographic orientation aligned with the direction of solidification, which can lead to anisotropic plastic behaviour (Terhaar et al., 2012). Chemical segregation and different mechanical behaviour of the phases composing dendritic and inter-dendritic grains can also lead to flow localisation and to heterogeneous recrystallisation (Han et al., 2013). Thus, the evaluation of the thermo-mechanical path and the evolution of the microstructure during the ingot-to-billet conversion process of the as-cast material remains challenging and consequently impedes the design and optimisation of the industrial manufacturing process.

This study aims to describe the mechanical and microstructural behaviours of the as-cast type 316 austenitic stainless steel through small-scale hot compression tests on samples extracted from an ingot. The objective is to point out the challenges and complexities introduced by the as-cast microstructure on the mechanical properties and microstructure evolution.

2 Material

The present investigations are focused on a Niobium-stabilised type 316Nb austenitic stainless steel with nominal chemical composition of 0.075C, 18Cr, 12Ni, 0.6Nb, 65Fe, 0.4Si and 1.1Mn, in wt %. An as-cast ingot with ≈ Ø 185 x 550 mm dimensions was produced through consecutive vacuum induction melting (VIM) and vacuum arc re-melting (VAR) at *Aubert & Duval*. The solidification microstructure of the ingot along transverse and longitudinal sections is shown in Fig.1 a). The as-cast structure is composed of coarse, elongated grains oriented predominantly radially at ≈ 60° from the axis of the ingot although grains at the core of the ingot are aligned with the axis. This appearance depends on the cooling rates and progression of re-melting (Kou, 2003). Cylindrical samples for upsetting tests were extracted by Electro Discharge Machining (EDM) from the as-cast ingot, and machined to final dimensions. As shown in Fig.1 a), the samples are described as axial and radial with their axis parallel and perpendicular to the axis of the ingot, respectively, to study the influence of the upsetting direction with respect to the as-cast grain orientation. Their respective microstructures are presented in Fig.1 b) and c). The samples had dimensions of Ø 60 x 60 mm to reduce the effect of their structure on their deformation by increasing the number of grains/volume of material, and a 1:1 height to diameter ratio to limit their temperature gradient prior to non-isothermal upsetting tests.

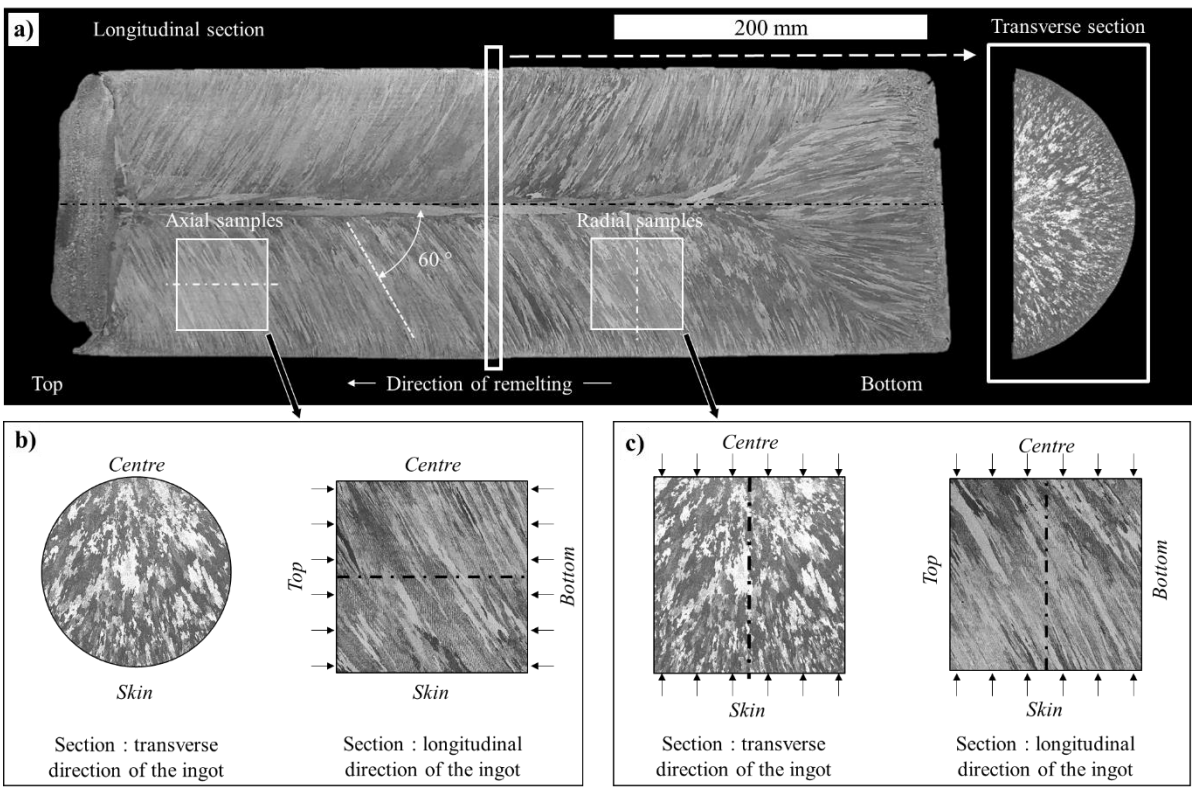

Fig.1: Microstructure of a) the as-cast VIM/VAR processed ingot, and of the cylindrical b) axial and c) radial samples taken out for upsetting tests, with the direction of upsetting indicated by arrows.

3 Methodology

3.1 Upsetting tests

All samples were subjected to different deformation levels by upsetting, to 17, 30, and 50% height reduction (upsetting) ratios. The axial samples were heated to 1100 and 1200°C prior upsetting, and the radial samples were only heated to 1200°C. A 500 Tons (T) capacity hydraulic press, controlled with a constant strain-rate of 0.1 s^{-1}, was used for the upsetting trials. The load applied by the press and the position of the upper ram were recorded during forging, with a resolution of 0.5 T and 0.5 mm, respectively. Lubrication with a mixture of water and graphite slurry was used as a lubricant were used to reduce the effect of friction between the samples and the dies during the trials. The samples were then quenched immediately after upsetting, to freeze their microstructures for subsequent analysis of the Dynamic Recrystallization (DRX).

3.2 Microstructural analysis

The deformed samples were cut along their longitudinal axis and prepared for light Optical Microscopy (OM) using standard metallographic sample preparation techniques. The microstructures were revealed by electro-etching using 10% (wt) oxalic acid as electrolyte and by applying 6 volts, as per ASTM E407-197. OM micrographs were collected at ×5 magnification, and stitched together to reconstruct the full cross-sectional image of the deformed samples. Each micrograph represent a 1.9 × 2.5 mm zone. The grain and grain boundaries are detected using an in-house watershed segmentation routine developed in Matlab® R2018a. Recrystallised and non-recrystallised grains were identified on each micrograph by defining a grain surface area threshold below which they are considered as recrystallised, and the average fraction of recrystallised grains in the micrograph was measured. The process is repeated for each micrograph, and the results were exported as large single images, giving an overview of the progress of recrystallisation in the samples.

3.3 FE analysis

A FE model was developed in the commercial FE software Forge® NxT 3.0 by Transvalor® to describe the upsetting trials. The transfer time and holding/dwelling duration used in the FE model were those measured during the testing. The kinematic behaviour of the dies during forging simulation was based on that recorded by the press. The material behaviour was modelled by the simplified Hansel-Spittel thermo-viscoplastic law, presented in equation (1), with the parameters given by Forge® database for the AISI 316 Nb, given in Table 1.

$$\sigma = A \cdot e^{m_1 T} \cdot \varepsilon^{m_2} \cdot \dot{\varepsilon}^{m_3} \cdot e^{\frac{m_4}{\varepsilon}} \quad (1)$$

Table 1 : Values of the parameters of the simplified Hansel-Spittel equation given by Forge® database for the AISI 316 Nb.

Parameter	A	m_1	m_2	m_3	m_4
AISI 316 Nb	4660.0156	-0.00311	-0.09996	0.09794	-0.06481

The orthotropic Hill-48 yield criterion (Hill and Orowan, 1948) was implemented into the FE model to account for the material's plastic anisotropic behaviour. Assuming that the anisotropy was related to the preferential orientation of the grains, the anisotropy axis were defined as shown in Fig. 2 a), where the axis "A3" was aligned with that of the grains. To consider the symmetry of microstructure evolution around the axis of the ingot, and therefore that of the system of the anisotropy axes, a dedicated user-variable routine developed by Transvalor® was used in the FE model. A marking grid aligned with the orientation of the microstructure is also implemented into the FE model to evaluate its deformation during forging, according to Fig. 2 b).

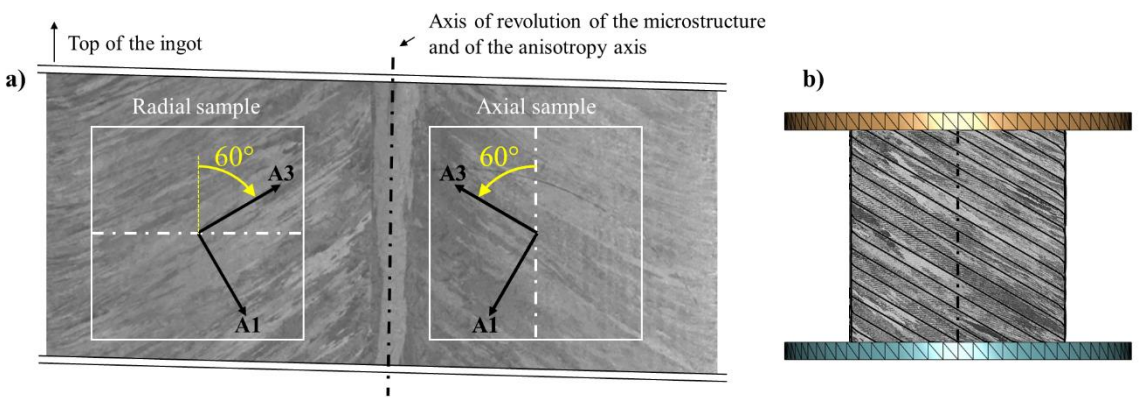

Fig. 2: Consideration of the material microstructure in the FE model: a) definition of the anisotropy axis and b) implementation of a marking grid for an axial sample, according to the orientation of the microstructure.

The expression of the Hill-48 yield criterion is given by equation (2). The set of parameters required to describe the anisotropic plastic behaviour, defined by a "trial and error" approach so that the shape of the samples matched with that predicted by the simulation.

$$\sigma_0{}^2 = F \cdot (\sigma_{22} - \sigma_{33})^2 + G \cdot (\sigma_{11} - \sigma_{33})^2 + H \cdot (\sigma_{11} - \sigma_{22})^2 + 2L \cdot \sigma_{23}{}^2 + 2M \cdot \sigma_{13}{}^2 + 2N \cdot \sigma_{12}{}^2 \quad (2)$$

After optimisation, the parameters F, G, H, L, M and N, which describe adequately all upsetting ratios, were found to be those presented in Table 2.

Table 2 : Values of the parameters of the Hill-48 yield criterion.

Parameter	F	G	H	L	M	N
Isotropic behaviour	0.5	0.5	0.5	1.5	1.5	1.5
Current anisotropic behaviour	0.5	0.5	0.5	0.675	0.675	1.5

4 Results and discussions

4.1 Geometry of the samples after forging

Example of samples after forging are presented in Fig. 3. The deformed samples have a non-axisymmetric shape, and owing to the anisotropic plastic behaviour of the as-cast material. The irregularities on their surface can be ascribed to the coarse grain size. The lateral surface of the samples forged with the highest upsetting ratio of 50% is shown to fold on the surface of the dies during forging.

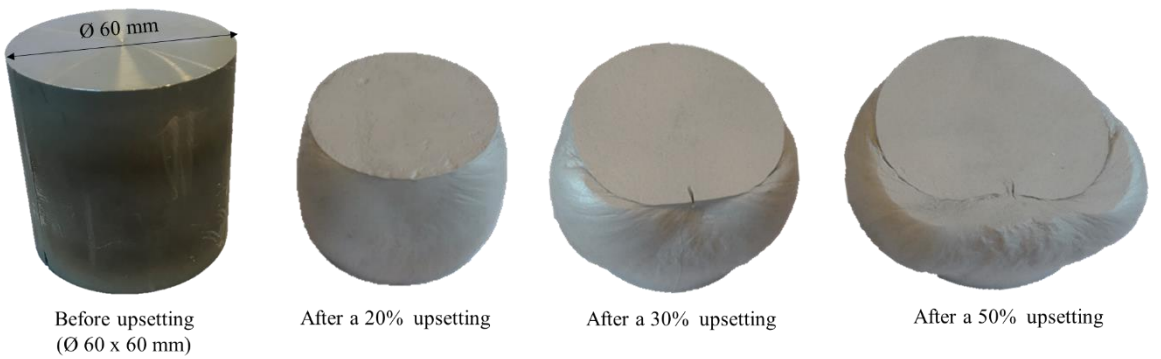

Fig. 3: Radial samples before and after forging to the indicated upsetting ratios. Dimension of the samples before forging : Ø 60 x 60 mm.

4.2 Data recorded by the press: forging loads and upsetting ratios

The data recorded by the press during upsetting of the axial and radial samples are presented in Fig. 4 a) and b), respectively. The experimental process shows a good repeatability; the experimental data obtained for each condition, including temperatures and samples orientations, overlap regardless of the upsetting ratio. This demonstrates the advantage of using large-size samples with regard to the representative microstructure and volume for the investigation on the as-cast material. A small deviation of the load recorded for the radial sample forged to a 20% upsetting ratio cannot be explained using the existing data. Axial and radial samples appear to require a similar forging load (≈ 80 T), although the orientation of their initial microstructures and the direction of the applied load were different.

Despite of the specific rotational symmetry of the initial microstructure, the respective microstructure of the samples had significant differences. It is therefore more than likely that the tests carried out on these samples are not able to capture the grain orientation dependency of the tests. The material behaviour is similar for the two main directions (i.e., radial and axial) which depend mainly on the size and alignment of grains, rather than purely grain orientation (Semiatin et al., 2004).

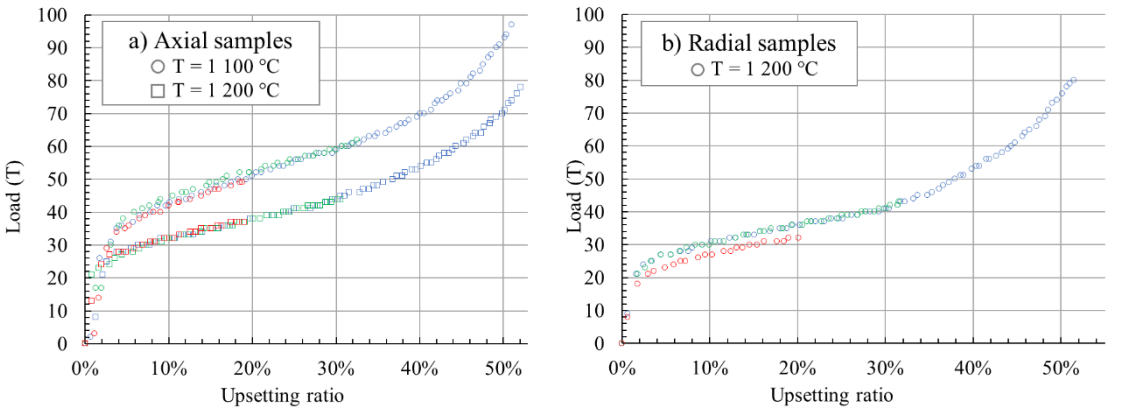

Fig. 4: Experimental load-position data: a) axial, and b) radial samples.

4.3 Anisotropic FE model of Upsetting

3D meshes of the samples after forging were generated by stereovision using an ATOS III ScanGOM system. Using the commercial software GOM Inspect®, the average absolute surface deviation between the surfaces of the samples after forging and that predicted by the FE model was evaluated. The shear angle of each sample, which is the angle between the direction of upsetting and the line joining the centre of their lower and upper surfaces, was measured. The results obtained for the axial and radial samples heated to 1200°C prior to 30% upsetting are presented in Fig. 5 a) and b), respectively. A good correlation between experimental and FE results is shown, although the radial specimen presents high deviation along the edge of the upper and lower surfaces of the sample. This deviation between experimental and FE results of the radial sample can be ascribed to the occurrence of shear deformation during upsetting, revealed by the high value of shear angle, seven times higher than that measured for the axial sample. The shear deformation behaviour is not predictable by the FE model, which explains the high local surface deviation shown in Fig. 5 b).

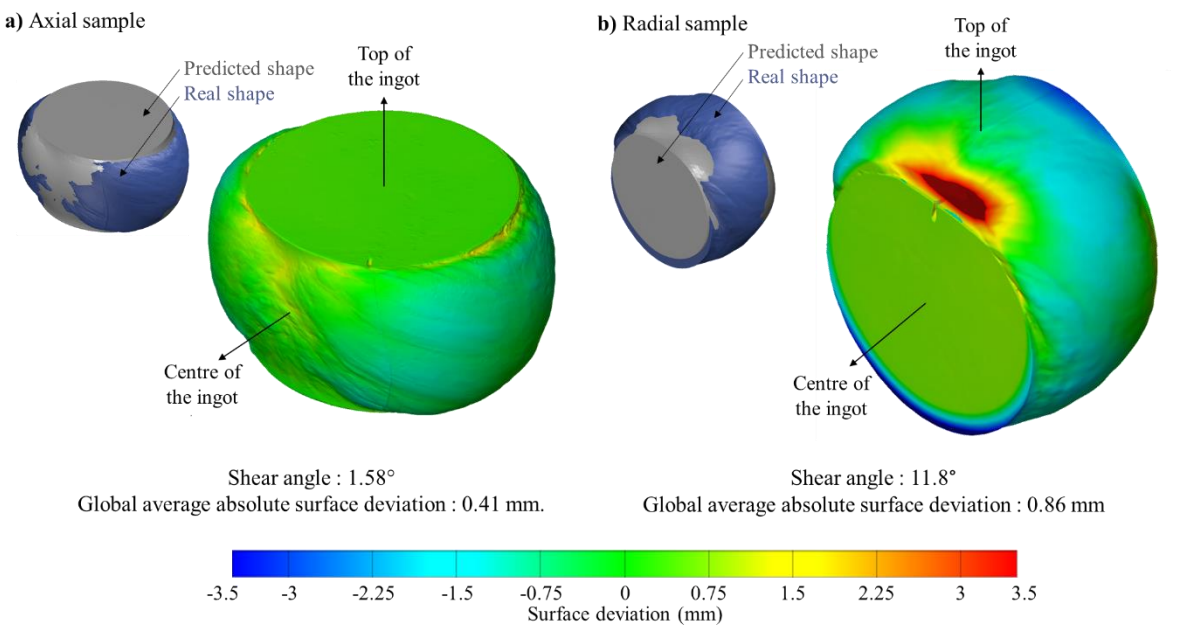

Fig. 5: Surface deviation of the FE results to the shape of the samples after forging: a) axial sample and b) radial sample. Heating temperature: 1200°C, Upsetting ratio: 30%.

These results demonstrate the capability of the FE model to predict the deformation of the samples using the orthotropic Hill-48 yield criterion, although the set of parameters have been defined by a "trial and error" approach. Investigation reported in the literature on coarse and elongated solidification microstructure have shown the

anisotropic plastic deformation of as-cast material can either result from the preferential crystallographic texture, or from the specific geometrical distribution of the microstructure (Park et al., 2005; Semiatin et al., 2004). However, the respective contribution of these two aspects have not been investigated in the present study.

Since the FE model is able to predict the deformation and shape of the samples during forging (Fig. 5), the equivalent plastic strain maps in the sample was evaluated with a reasonably high confidence level. The FE results given for the isotropic case are presented in Fig. 6 a), and the anisotropic cases are presented in Fig. 6 b) and Fig. 6 c) for the axial and radial samples, respectively. The maximal value of the macroscopic equivalent plastic strain, reached for the anisotropic cases, is about 40% higher than that predicted for the isotropic case, and its distribution is also affected by the orientation of the sample. This demonstrates the need to consider the anisotropic plastic flow of the as-cast material in the FE models to enhance the accuracy of the prediction. By comparing the deformation of the marking grid, initially aligned with the material microstructure, and the strain maps in Fig. 6 b) and Fig. 6 c), it can be observed that a relatively high strain gradient can take place in the width of one single grain.

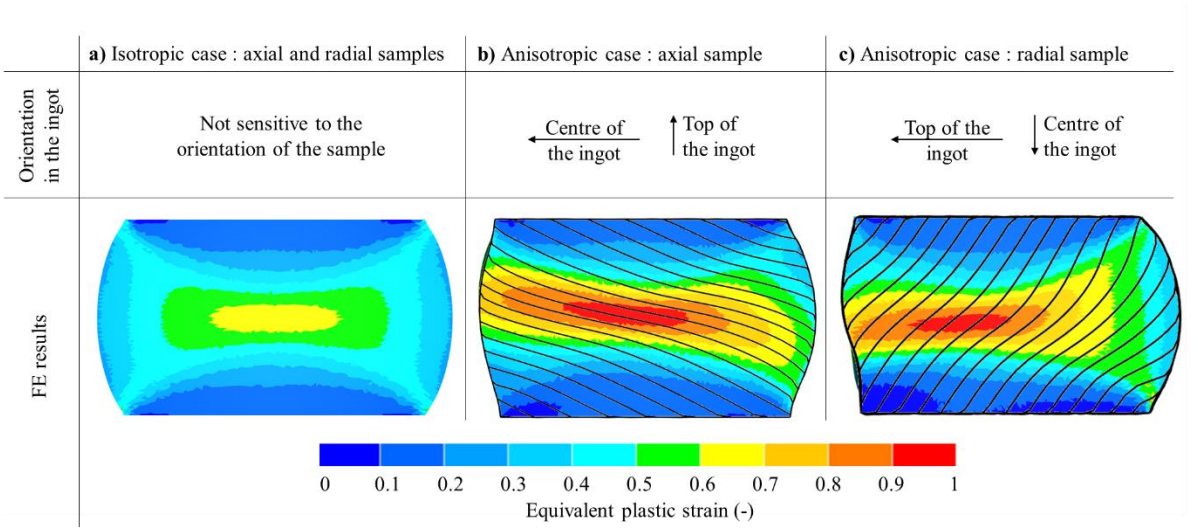

Fig. 6: Results of FE simulations for the axial and radial samples heated to 1200°C prior to a 30% upsetting, with and without consideration of the anisotropic plastic behaviour. Results are displayed on the longitudinal section of the samples that also corresponds with that of the as-cast ingot. The upsetting axis is aligned with the vertical direction.

4.4 Microstructure evolution and correlation with the FE results

Representative micrographs to show the microstructural evolution in the samples is presented in Fig. 7. It can be seen that recrystallised grains are heterogeneously distributed in the sample after upsetting. The nucleation sites of the recrystallised grains are located either at the grain boundaries or at the interface with the secondary phases, which is in line with the results reported in the literature for as-cast microstructures (Hermant et al., 2019; Mandal et al., 2012; Mataya et al., 2003).

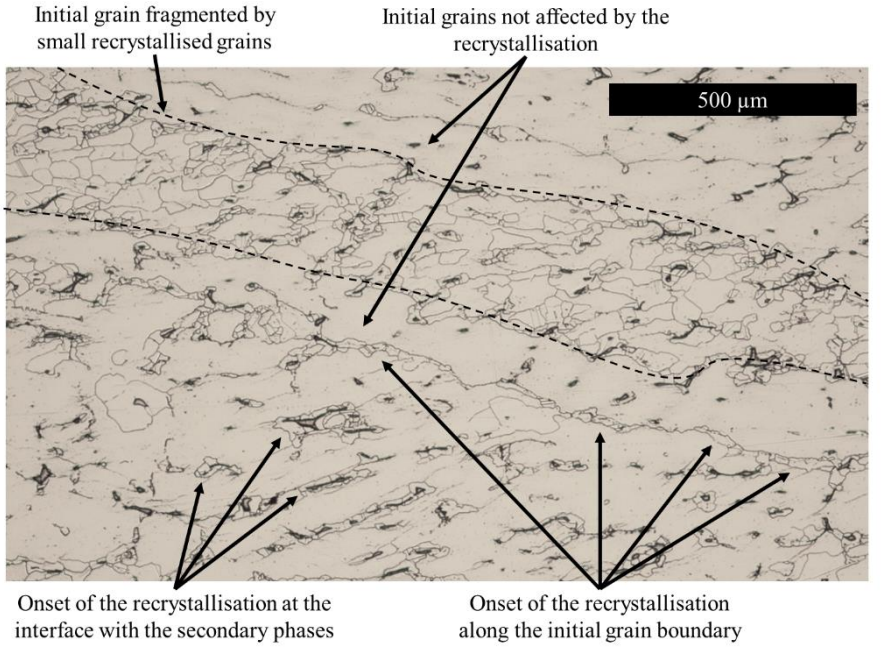

Fig. 7: Micrograph taken at the core of a sample heated at 1200°C and forged to the upsetting ratio of 20%, describing the evolution of the material microstructure : nucleation of the grains at the interface with the secondary phases or at the grain boundaries, and presence of preferentially-recrystallised grains.

Correlation of the recrystallised microstructure with the FE results is presented in Fig. 8 for the axial samples heated to 1200°C prior forging to the intermediate upsetting ratio of 30%. Observation of the microstructure and the location of the recrystallised grains in Fig. 8 a) shows that recrystallisation occurs along strip-wise regions termed as "recrystallised bands", which are oriented along the marking grid resulting from the FE simulation. This is consistent with the micrographs presented in Fig. 7. Recrystallisation is also more pronounced in the core of the sample, where high temperature (Fig. 8 b)) and equivalent plastic strain values (Fig. 8 c)) are predicted by the FE model.

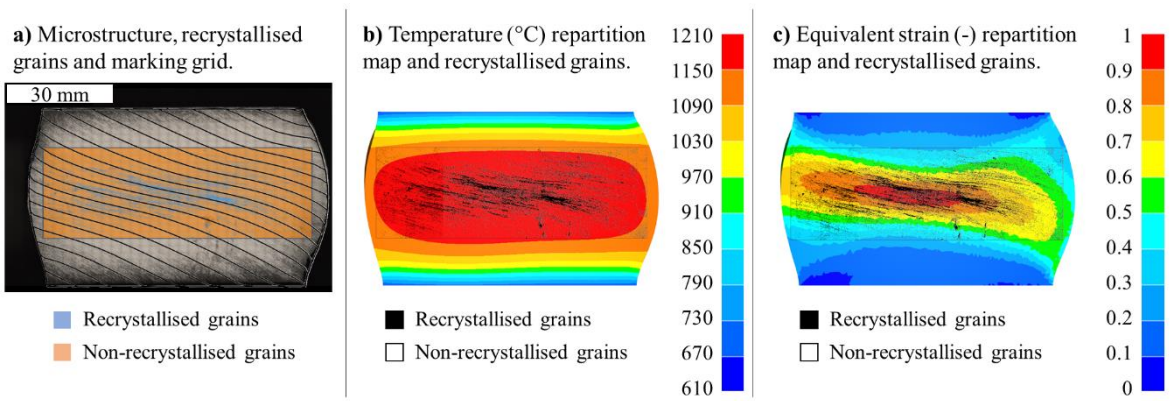

Fig. 8: Experimental identification of the recrystallised grains in the samples, overlaid on a) the temperature, b) the structure of the samples and c) on the equivalent strain distribution predicted by the FE model. Axial sample forged at 1200°C to a 30% upsetting ratio.

These results are confirmed by the measurements of the fraction of recrystallised grains presented in Fig. 9 for the samples heated to 1200°C prior to upsetting. The progress of the recrystallisation throughout the forging process depends on strain and temperature levels, but also on the size and orientation of the initial grains in the microstructure of the samples. However, the recrystallisation remains incomplete even in the central region of the samples and the presence of the "recrystallised bands" suggest the occurrence of flow localisation. This can lead to local strain heterogeneities and additional recrystallisation-induced anisotropy, occurring with the progress of the DRX during the deformation of the sample. This phenomenon is ascribed to the coarse elongated microstructure of

the material, and is not predictable by the FE model. Thus, evaluation of usual Johnson-Mehl-Avrami-Kolmogorov (JMAK) type equation for DRX using FE model is limited for the present material microstructure.

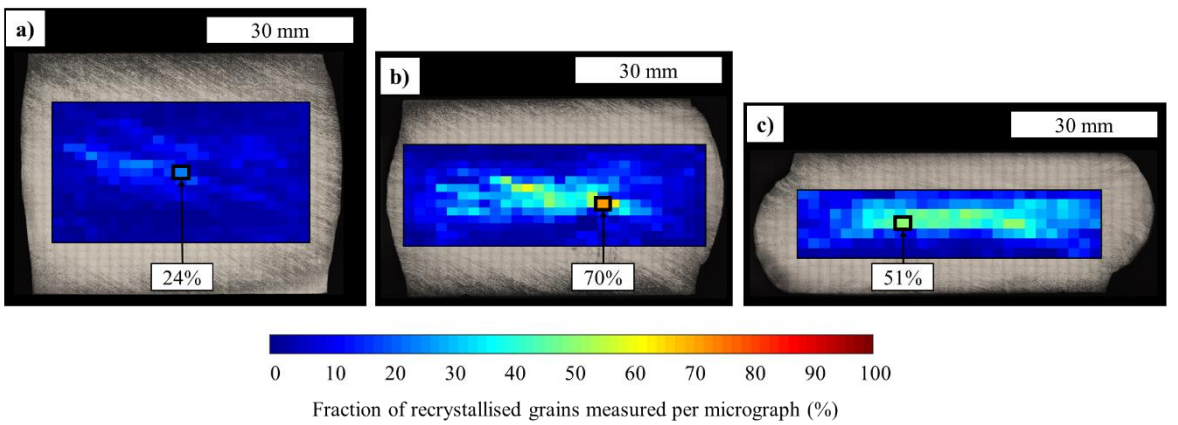

Fig. 9: Measurements of the fraction of recrystallised grains in the samples heated to 1200°C prior to upsetting. The values reported in the figure corresponds to the highest measurement of the fraction of recrystallised grain.

5 Conclusion and outlook

In the present study, the as-cast material behaviour of Ø 60 x 60 mm samples taken out from a VIM/VAR processed ingot of AISI 316 Nb was investigated. The evolution of the microstructure was measured, and a FE model has been developed to predict the deformation of the samples during the upsetting tests. The following conclusions were drawn:

- The recrystallised grains are either located at the grain boundaries or at the interface with the secondary phases, and are aligned along “recrystallised bands” having the same orientation as the initial microstructure.
- The conditions involved in the upsetting tests, i.e.: 50% upsetting at 1200°C, did not permit the complete recrystallisation of the as-cast microstructure. Thus, forging paths involving multi-directional deformations of the material and intermediate annealing heat treatment are required during the ingot-to-billet manufacturing process.
- The global anisotropic plastic deformation of the as-cast material can be ascribed to the orientation of its specific solidification microstructure. It is implemented in a FE model to predict with a good accuracy the shape of the samples after forging, and demonstrate its non-negligible impact on the equivalent plastic strain levels and repartition in the samples. This must therefore be considered in the design process of the ingot-to-billet manufacturing routes.

Following the present work, further investigation are required to enhance the definition and the optimisation of ingot-to-billet manufacturing routes:

- Quantitative measurements of the fraction of recrystallised grains after multi-directional forging and subsequent heat treatments are required to consider the effects of the thermal cycles involved during the industrial process on the evolution of the microstructure.
- Cogging and upsetting industrial-scale ingots and subsequent analysis are required to evaluate the representativeness of the results obtained from the present work, using small-scale samples.
- A CPFEM-based model can be developed to define more precisely the value of the Hill’s parameters used in FE models. This would also permit to investigate on the sensibility of the material behaviour regarding the orientation of the solicitation, and to evaluate the respective contribution of the crystallographic and geometric orientation of the microstructure to the anisotropic plastic behaviour of the as-cast material.
- Determination of the material flow stress, and its dependence to temperature and strain, is required for the development of accurate and predictive FE models. The current method for the determination of the stress-

strain curves using results of upsetting tests are based on axisymmetric deformation, and further improvements are required to comply with anisotropic plastic deformation of the samples.

6 Acknowledgements

Authors gratefully acknowledge Stephen MICHIE, Stephen WAUGH, Lee MCGARRY, Kornelia KONDZIOLKA, Sébastien NOUVEAU, Jean-Baptiste MAILLET, and Emile DELAUNAY for their technical support and advice in carrying out this work.

7 References

Antolovich, B.F., Evans, M.D., 2000. Predicting Grain Size Evolution of Udimet Alloy 718 during the " Cogging " Process through Use of Numerical Analysis. Presented at the Superalloys 2000.

Han, Y., Liu, G., Zou, D., Liu, R., Qiao, G., 2013. Deformation behavior and microstructural evolution of as-cast 904L austenitic stainless steel during hot compression. Materials Science and Engineering: A 565, 342–350. https://doi.org/10.1016/j.msea.2012.12.043

Han, Y., Wu, H., Zhang, W., Zou, D., Liu, G., Qiao, G., 2015. Constitutive equation and dynamic recrystallization behavior of as-cast 254SMO super-austenitic stainless steel. Materials & Design 69, 230–240. https://doi.org/10.1016/j.matdes.2014.12.049

Hermant, A., Suzon, E., Petit, P., Bellus, J., Georges, E., Cortial, F., Sennour, M., Gourgues-Lorenzon, A.-F., 2019. Hot Deformation and Recrystallization Mechanisms in a Coarse-Grained, Niobium Stabilized Austenitic Stainless Steel (316Nb). Metall and Mat Trans A 50, 1625–1642. https://doi.org/10.1007/s11661-018-05103-x

Hill, R., Orowan, E., 1948. A theory of the yielding and plastic flow of anisotropic metals. Proceedings of the Royal Society of London. Series A. Mathematical and Physical Sciences 193, 281–297. https://doi.org/10.1098/rspa.1948.0045

Jonas, J.J., Quelennec, X., Jiang, L., Martin, É., 2009. The Avrami kinetics of dynamic recrystallization. Acta Materialia 57, 2748–2756. https://doi.org/10.1016/j.actamat.2009.02.033

Kou, S., 2003. Welding metallurgy, 2nd ed. ed. Wiley-Interscience, Hoboken, N.J.

Mandal, G.K., Stanford, N., Hodgson, P., Beynon, J.H., 2012. Effect of hot working on dynamic recrystallisation study of as-cast austenitic stainless steel. Materials Science and Engineering: A 556, 685–695. https://doi.org/10.1016/j.msea.2012.07.050

Mataya, M.C., Nilsson, E.R., Brown, E.L., Krauss, G., 2003. Hot working and recrystallization of As-Cast 316L. Metall and Mat Trans A 34, 1683–1703. https://doi.org/10.1007/s11661-003-0313-8

Park, N.-K., Yeom, J.-T., Kim, J.-H., Cui, X.-X., 2005. Characteristics of VIM/VAR-Processed Alloy 718 Ingot and the Evolution of Microstructure During Cogging, in: Superalloys 718, 625, 706 and Various Derivatives (2005). Presented at the Superalloys, TMS, pp. 253–260. https://doi.org/10.7449/2005/Superalloys_2005_253_260

Semiatin, S.L., Weaver, D.S., Kramb, R.C., Fagin, P.N., Glavicic, M.G., Goetz, R.L., Frey, N.D., Antony, M.M., 2004. Deformation and recrystallization behavior during hot working of a coarse-grain, nickel-base superalloy ingot material. Metall and Mat Trans A 35, 679–693. https://doi.org/10.1007/s11661-004-0379-y

Terhaar, J., Poppenhäger, J., Bokelmann, D., Schafstall, H., Kelkar, K., 2012. Considering the solidification structure of VAR ingots in the numerical simulation of the cogging process. 7th International Symposium on Superalloy 718 and Derivatives 2010 1, 13. https://doi.org/10.1002/9781118495223.ch4